5-2021

Low Impact Development: Low-Maintenance Design to Encourage Residential Adoption of Sustainable Systems

Haley Ellis

LOW IMPACT DEVELOPMENT: LOW-MAINTENANCE DESIGN TO ENCOURAGE RESIDENTIAL ADOPTION OF SUSTAINABLE SYSTEMS

Haley Ellis

Biological Engineering Program

Biological and Agricultural Engineering Department

College of Engineering

University of Arkansas

Undergraduate Honors Thesis

This thesis has been approved by the Biological and Agricultural Engineering Department for submittal to the College of Engineering and Honors College at the University of Arkansas.

[redacted]

BENG Honors Advisor: Dr. Benjamin Runkle

[redacted]

Honors Committee Member: Dr. Brian Haggard

[redacted]

Honors Committee Member: Dr. David Miller

[redacted]

Departmental Honors Coordinator or Department Head

Contents

ABSTRACT **1**

INTRODUCTION **2**

PROJECT SCOPE AND OBJECTIVES 4

METHODS OF DESIGN **4**

SITE SELECTION 4

SOIL TESTING 7

SYNTHETIC STORMS AND SWMM PARAMETERS 7

SHANNON-WEINER DIVERSITY INDEX 16

RESULTS **17**

SOIL ANALYSIS 17

SWMM ANALYSIS 17

DIVERSITY INDEX ANALYSIS 21

DISCUSSION AND FUTURE OPPORTUNITIES **22**

CONCLUSION **25**

ACKNOWLEDGEMENTS **27**

REFERENCES **28**

APPENDIX A. WILDFLOWER SPECIES NATIVE TO NW ARKANSAS AND THE SOUTHERN PLAINS REGION **33**

APPENDIX B. 3D GOOGLE EARTH IMAGES OF LOCATION OF INTEREST **34**

APPENDIX C. RAIN BARREL EXFILTRATION **35**

APPENDIX D. SHANNON-WEINER DIVERSITY INDEX **36**

APPENDIX E. RAIN GARDEN RUNOFF PREDICTION **38**

Abstract

Residential adoption of low-impact development (LID) technology can positively impact downstream watershed hydrology by reducing total volumetric discharge from the residential site. This reduction can provide economic, environmental, and social benefits for the residents as well as the community at large. Additionally, homeowners are often affected by stormwater related issues, like flooding or washout, that could be easily mitigated with a sustainably engineered LID structure or network. Engineering for sustainability often includes the blending of several objectives to provide greater overall benefit. This thesis compares the outflow characteristics of three low-maintenance residential LID design scenarios differing in rain garden soil depth and therefore differing in available pore space. As pore space increases, water storage potential also increases, allowing for greater reductions in total volumetric discharge. Despite this relationship, the deepest possible rain garden cannot be considered the best choice for all homeowners. Economic considerations may deter some who are interested in environmental preservation but cannot endure the initial cost of investment attached to the most environmentally beneficial design. To encourage widespread adoption, it is recommended that homeowners invest in low-maintenance LIDs that incorporate the use of native plant species in the design. Generally, the incorporation of residential rain gardens provides exceptional benefit. These LIDs excel in the reduction of total volumetric discharge and can be designed to aesthetically appeal to a multitude of visual preferences. By following this guidance, homeowners can enjoy the benefits of successful and sustainable engineering design while also providing an ecological service to their community.

Introduction

Low Impact Development (LID) design techniques are often implemented in urban environments—with large-scale, community-wide benefits in mind—to control stormwater, reduce total volumetric or peak runoff, and improve water quality as it re-enters the hydrologic cycle. However, not enough emphasis is placed on the collective impact that can be made when small-scale, residential LIDs are constructed for the same purpose. This approach of reducing stormwater runoff at its source decentralizes mitigation techniques seen in traditional LID design. When used in series, LID technologies can better accomplish these goals.

By creating a network, such as collecting roof runoff in a rain barrel surrounded by a herbaceous field, conveying the water via vegetative swales, and retaining the water in a nearby rain garden, peak runoff can be reduced by up to 75% when compared with traditional sewer systems (Peng et al., 2019). Rain barrels alone have proven hardly effective in reducing runoff and are best used in combination with other technologies or for water conservation purposes (Jennings et al., 2013; Buchhorn, 2018). An Illinois survey indicated that most adopters of rain barrel technology are motivated by the additional water source and primarily use harvested rainwater for irrigation, reducing their reliance on treated tap water (Buchhorn, 2018). Vegetative swales have proven successful in the reduction of metals like zinc and iron through both infiltration and surface flow (Ismail et al., 2014); however, it is important to note that these structures do not adequately address nutrient removal. Furthermore, if sized appropriately, residential rain gardens can eliminate volumetric runoff through infiltration, significantly reducing downstream hydrologic impact (Abi Aad et al., 2010).

Many standard recommendations for rain garden construction suggest they be at least 20-30% the size of the drainage service area (sub-watershed area from which they receive runoff), which can be spatially limiting in the case of residential adoption. However, simulations show that a garden sized to only 5% of the service area can effectively reduce runoff by as much as 60%, even in the presence of

inappropriate soil conditions (Jennings et al., 2015). This study goes on to claim that "much of the current rain garden design guidance is unnecessarily conservative" and "nearly any rain garden of any depth and any size will have some beneficial impact," reporting simulated runoff reductions of up to 85% in the most conservative cases.

It is important to consider the working relationship between evapotranspiration (ET) and deep infiltration when engineering successful LIDs. ET can reduce volumetric runoff by as much as 84% (Hess et al., 2017), significantly reducing soil moisture content and promoting deep infiltration (Wadzuk et al., 2015). Engineering decisions like soil type (sandy or loamy, and whether the soil falls into hydrological soil group (HSG) A, B, C, or D), soil depth, and flow path will determine whether ET or deep infiltration is responsible for the bulk of reduction (DelVecchio et al., 2020). These parameters will also determine whether it is necessary to include an underdrain to avoid overflow (Mohammed et al., 2019). Soils high in clay (typically HSG D) will require underdrains while soils high in sand may not. "Quarrying and importing of sand" produces more greenhouse gas (GHG) emissions than any other part of a rain garden system (Flynn and Traver, 2013), so engineering for sustainability will likely include working with the naturally occurring soil types, if possible. However, when designing LIDs, it is most important that the element reduces or attenuates discharge; thus, importing sandy soils to accommodate this requirement is often necessary.

Public support for residential LID adoption is not necessarily a straightforward issue. For example, in Vermont, a statewide survey was conducted to determine the stormwater experiences of residents where 54% of the participants noted at least one encounter with erosion, flooding, washout, or another issue with stormwater runoff (Coleman et al., 2018). Despite this, "too much upkeep" is a commonly cited deterrent in the refusal to implement an LID solution. Intentionally designing a low-maintenance system could lead to a greater willingness to adopt this technology. Vegetation type has proven to have little effect on stormwater reduction; in fact, vegetation-free systems like rock gardens can be just as effective

as a highly vegetated system (Jennings et al., 2015). Therefore, encouraging homeowners to grow plants they find attractive and that require little to no maintenance in their hardiness zone may inspire further interest.

Generally, native plant species will require less maintenance and human intervention than species far outside their natural habitat. Therefore, incorporating native wildflower species in the design of a residential rain garden will ultimately reduce the need to maintain the structure, saving homeowners time and money. Some wildflower species can develop root systems reaching as deep as 4.5 m below the soil's surface, further increasing the soil's moisture storage capacity and reducing the risk of soil erosion (AGFC, 2021). Additionally, plant species diversity positively correlates to overall biodiversity as well as pollinator-specific biodiversity (Kral-O'Brien et al., 2021). Furthermore, soil microbial richness is well-known to be positively impacted by plant diversity (Liu et al., 2020), an added benefit of designing wildflower-rich LIDs. Generally, a homeowner in Northwest Arkansas has several options when choosing plant species, varying in blooming season, color, maximum height, and water needs (Appendix A).

Project Scope and Objectives

This thesis investigates and models LID technologies to capture precipitation runoff, redirect overland flow, and attenuate peak and volumetric discharge. An LID system was designed to capture downspout discharge in a rain barrel, redirect captured runoff to a nearby vegetative swale to avoid concrete walkways, and convey captured runoff to a backyard rain garden. The EPA's Storm Water Management Model (SWMM) software was used to model outflow characteristics and compare present-day and LID design scenarios. Specifically, three LID scenarios were considered, differing only in rain garden soil depth, and subsequently, available pore space, to determine optimal conditions for runoff reduction.

Methods of Design

Site Selection

The area of interest includes the residential lot located in Washington County at 524 N Storer Ave, Fayetteville, AR 72701 with coordinates 36.071 °N, 94.172 °W (Figure 1); additional Google Earth images

are available in Appendix B. The local watershed has an approximate area of 2 km^2 with land uses including primarily developed, open space (52.4%), and developed, low intensity (34.2%) (Stroud Water Research Center, 2020). More than 56% of the soil within the area is classified as Type D – Very Slow Infiltration. Class D soils have high runoff potential when saturated and water movement through the soil is restricted (Werner et al., 2007). Soils in this HSG generally consist of more than 40% clay and less than 50% sand, forming a clayey texture. The terrain is varied with a minimum slope of 0%, maximum slope of 26.8%, and an average slope of 8.2%.

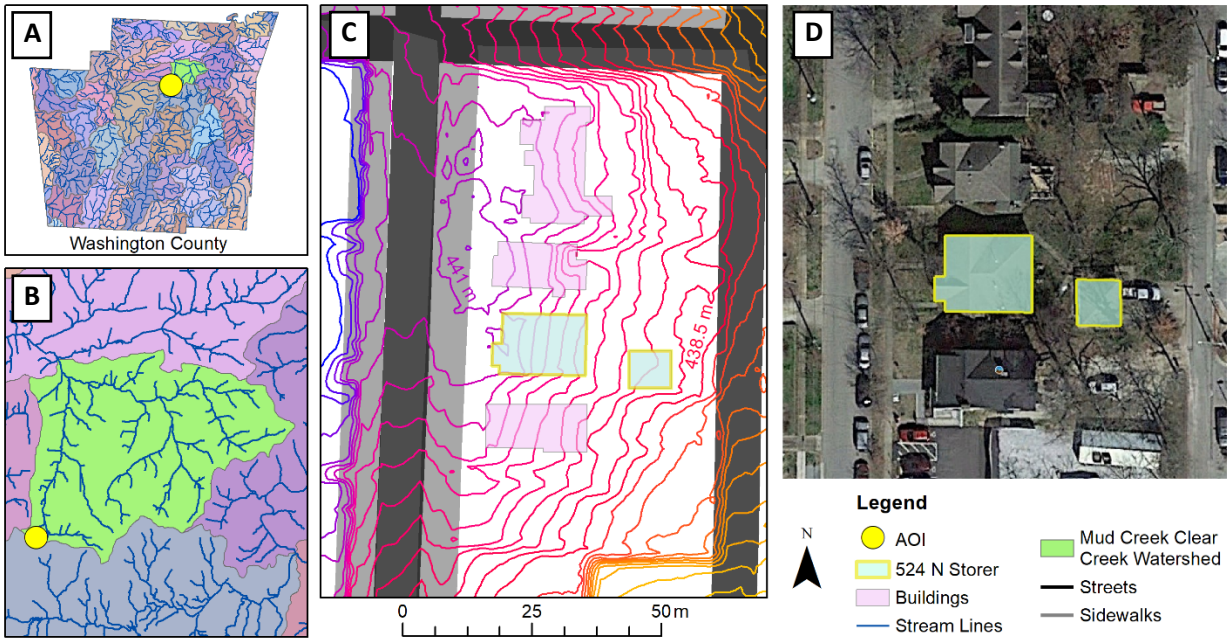

Figure 1. ArcMAP representation of location of interest; Washington County HUC-12 watersheds at scale 1:1,250,000 (A), Mud Creek Clear Creek Watershed at scale 1:180,000 (B), Location of interest at scale 1:1000 (C), and Google Earth image of location of interest (D). Sources include Arkansas GIS Office (2020), City of Fayetteville (2021), Earth Science Information Center (2013, 2019), Google Earth (2021), USDA-NRCS et al. (2015), and USGS (2020). 3D Google Earth images are available in Appendix B.

This study consists primarily of the northern half of the property—the southern half of the property has a separate discharge point and is therefore not included in this design. However, due to the shape of the property and location of downspouts, some portions of the southern half are included to ensure a comprehensive analysis. The existing layout of the property allows for runoff conveyance along the concrete walkway (Figure 2), which is both a hazard and an inconvenience for the residents. Runoff flows

both from a local high point, NW of the property, and from the residential downspouts. In particular, the downspout located on the NW corner of the residence directs roof runoff onto the paved walkway where it is conveyed underneath an existing side-porch culvert and into the backyard. The overland flow path is approximately 50 m long and consists of a 2.75-m change in elevation between the nearest high point, NW of the property line, and the discharge outlet point located on the eastern edge of the property (Figure 3). Discharge then flows northeast to Scull Creek where it enters the Mud Creek Clear Creek watershed (Stroud Water Research Center, 2020).

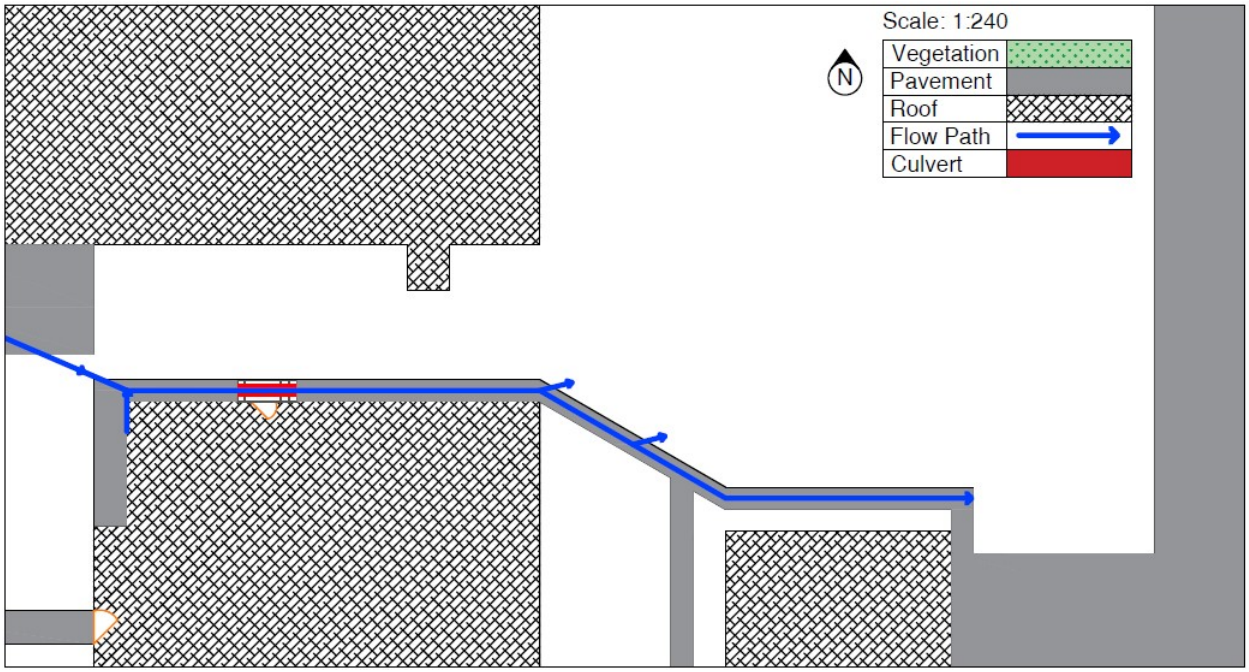

Figure 2. Overland flow path (outlined in blue) of present-day scenario. Water flows from a high point NW of the property and from a downspout attached to the NW corner of the home. Water is conveyed along the residential footpath where it then flows into the backyard. Runoff eventually exits at the eastern border of the property. Scale of 1:240 in units of meters.

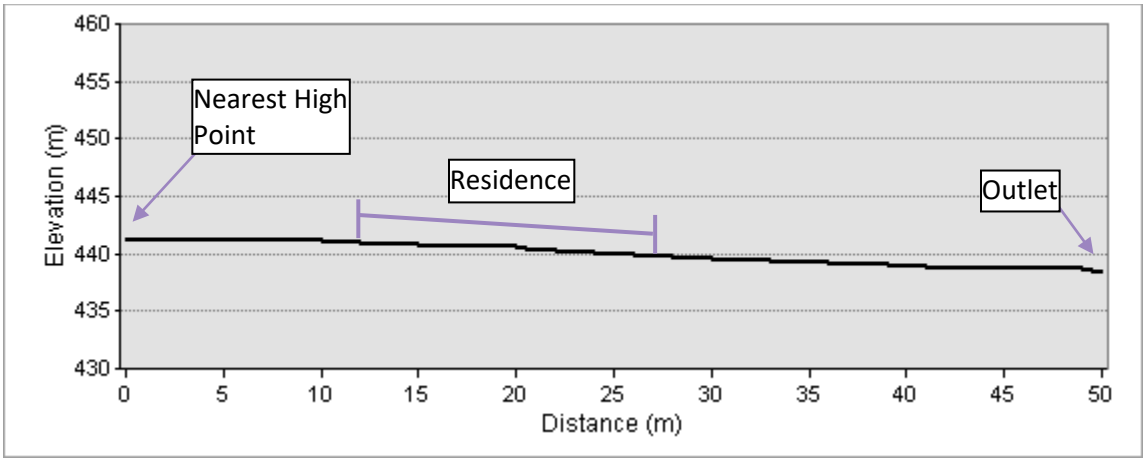

Figure 3. Area of interest elevation profile. Overland flow travels a distance of 50 m and descends approximately 2.75 m in elevation from the nearest high point (NW of residence) to the property outlet (eastern border). Elevation profile developed with ArcMAP (USGS, 2020). Y-axis elongated to show detail.

Soil Testing

To successfully evaluate present-day conditions, soil properties are essential in determining accurate runoff characteristics. Specifically, it is necessary to understand these properties when designing rain gardens to determine whether the importing of a more suitable soil type is required. Twelve samples were collected from the area of interest and examined to determine texture, gravimetric moisture content (θ_g), bulk density (ρ_b), volumetric moisture content (θ_v), and soil porosity. Soil texture was determined using the hydrometer method, calibrating for buoyancy and temperature (Backus, 2020). Gravimetric moisture content was calculated by oven-drying the samples and comparing the change in weight. This parameter allows for the calculation of soil bulk density which, in turn, allows for the calculation of volumetric moisture content and soil porosity.

Synthetic Storms and SWMM Parameters

Rainfall amounts for 24-hour design storms were considered for the 1-, 2-, 5-, 10-, and 25-year recurrence intervals as per the City of Fayetteville (2014) drainage design standards (Figure 4). These design storms represent total cumulative depths of 89 mm, 100 mm, 118 mm, 135 mm, and 159 mm, respectively (NOAA, 2021). Maximum intensity occurs at the 9-h time-step for all storms, measuring 4.86 mm/h, 5.46 mm/h, 6.44 mm/h, 7.37 mm/h, and 8.68 mm/h, respectively.

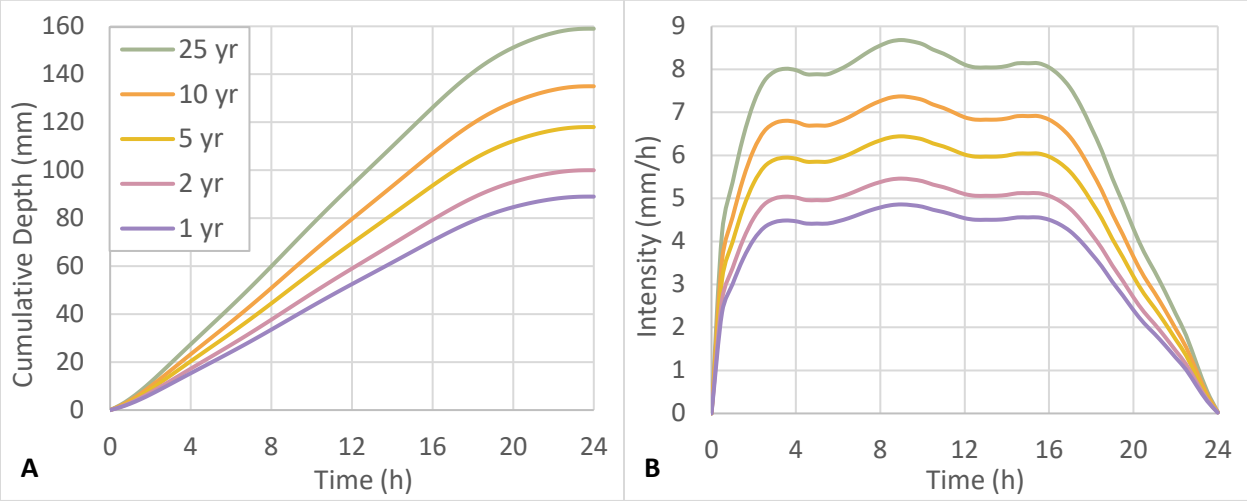

Figure 4. Hyetographs for 24-hour design storms. (A) Cumulative depth represents 50% occurrence for median across all storms. (B) Intensities developed using 30-min time increments (NOAA, 2021).

To determine discharge from the area of interest, SWMM parameters were adjusted to employ the Curve Number Infiltration Method, reporting at 30-min time intervals for 36 hours to accommodate post-storm runoff. The site was divided into eight sub-areas to evaluate the base scenario, all flowing to a common outlet at the eastern edge of the property (Figure 5). Sub-areas A, B, C, D, and E represent the impervious roof surfaces of the site of interest, including the garage (D), and half of the roof area of the northern neighbor (E). The inclusion of the northern neighbor's home was necessary because their residence possesses three downspouts that convey runoff into sub-area G. Sub-areas F, G, and H represent the front yard, side yard, and back yard of the residence, respectively. Sub-area characteristics are summarized in Table 1.

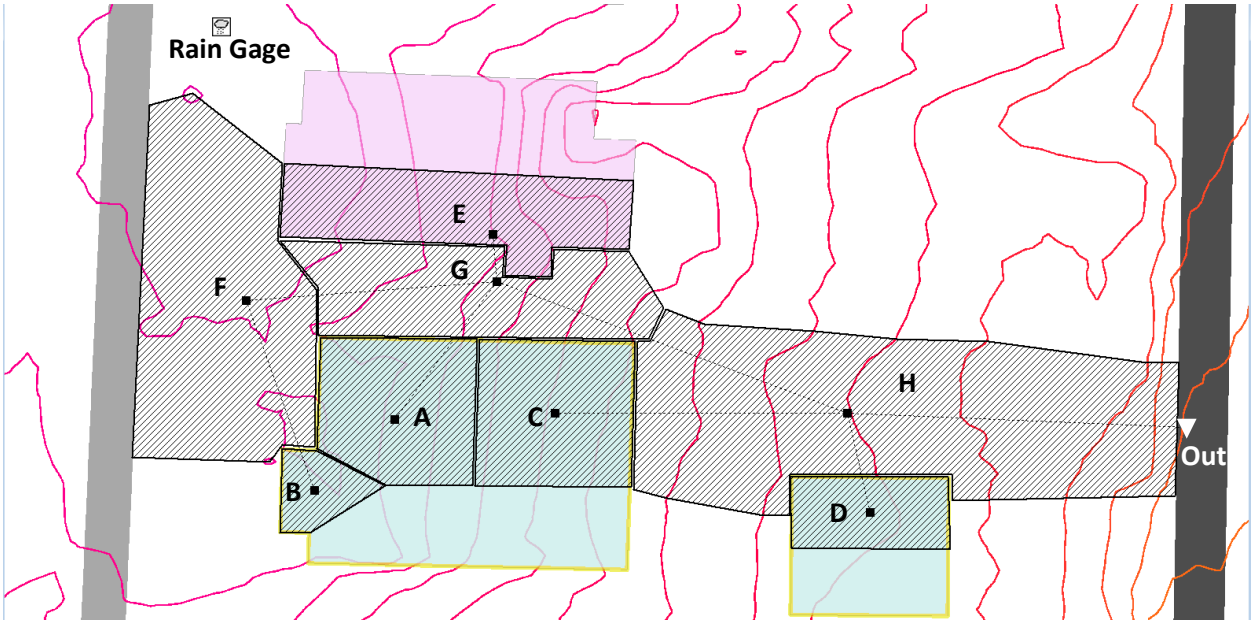

Figure 5. Base scenario land use sub-areas. Distance between roads measures approximately 54 m. Topographic lines represent 0.25-m contours. Labeled sub-areas and properties are detailed in Table 1.

Table 1. Sub-area parameters used as inputs in Base Scenario SWMM project.

Sub-Area	Outlet	Area (ha)	Width (m)[a]	% Slope[b]	% Imperv	N-Imperv[c]	N-Perv[d]	Subarea Routing[e]	% Routed[f]	HSG[g]	CN[h]
A	G	0.005	4.97	41.7	100	0.016	---	Outlet	---	---	98
B	F	0.001	1.84	41.7	100	0.016	---	Outlet	---	---	98
C	H	0.005	5.75	41.7	100	0.016	---	Outlet	---	---	98
D	H	0.002	3.96	41.7	100	0.016	---	Outlet	---	---	98
E	G	0.006	11.27	41.7	100	0.016	---	Outlet	---	---	98
F	G	0.01	10.40	5.2	40	0.012	0.15	Pervious	85	C	90
G	H	0.01	6.56	9.8	25	0.012	0.15	Outlet	---	C	90
H	Out	0.02	8.81	7.2	10	0.012	0.15	Pervious	100	D	92

a. Characteristic width of overland flow path.
b. Slopes for sub-areas A-F represent estimated roof pitch of 5/12. Slopes for sub-areas F-H represent calculated values of change in elevation versus distance between high point and low point.
c. Manning's roughness coefficient of sub-area impervious surface. Sub-areas A-E represent asphalt shingles with an assumed roughness coefficient equal to that of rough asphalt (City of Fayetteville, 2014). Sub-areas F-G represent greenspace. Impervious surfaces consist of smooth concrete. Roughness coefficient acquired from the EPA SWMM (2020) software index.
d. Manning's roughness coefficient of sub-area pervious surface. Pervious surfaces consist of short, prairie grass. Roughness coefficient acquired from EPA SWMM (2020) software index.
e. Internal routing classification. "Outlet" routes runoff directly to the subcatchment outlet. "Pervious" routes runoff from impervious surfaces to pervious surfaces. Some runoff is lost to infiltration and depression storage (US EPA et al., 2009).
f. Indicates percent of runoff internally routed.
g. Hydrologic Soil Groups based on soil testing results (Ross et al., 2018).
h. Curve Numbers for sub-areas A-E acquired from EPA SWMM (2020) software index. Values for sub-areas F-H determined through soil analysis.

To evaluate each LID scenario, three additional sub-areas were used to model the LID technologies. The LID sub-areas include a rain barrel (RB), two vegetative swales (VS1 and VS2), and a rain garden (RG) (Figure 6). The LID system is designed to capture roof runoff (in sub-area RB) from sub-area A, convey that runoff through VS1 and VS2, avoiding all concrete walkways and footpaths, and deposit the runoff into RG. Parameters for the existing sub-areas are unchanged except for area reductions in sub-area F, G, and H. This reduction in area for the non-LID sub-areas accounts for the area added with the addition of each LID technology. Newly calculated areas, as well as all other parameters, are summarized in Table 2.

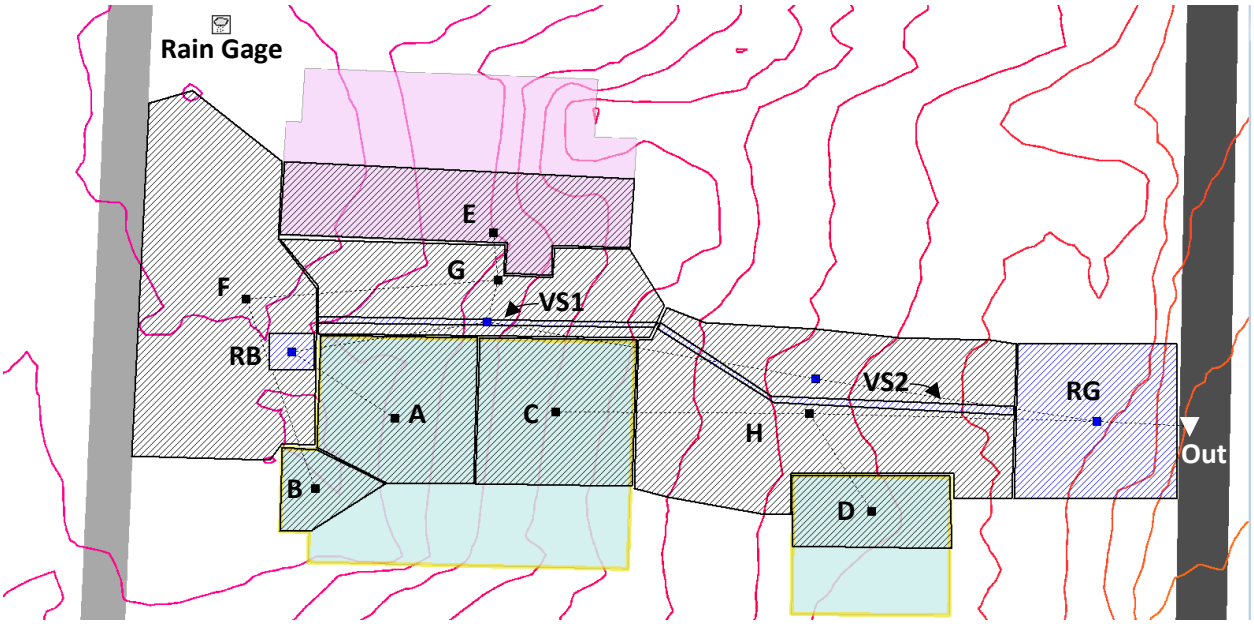

Figure 6. LID Scenario sub-areas. Distance between roads measures approximately 54 m. Topographic lines represent 0.25-m contours. LID sub-areas are shaded blue. Labeled sub-areas and properties are detailed in Table 2.

Table 2. Sub-area parameters used as inputs in SWMM for all LID scenarios. Sub-area A is newly routed to LID sub-area RB while all other parameters are unchanged. Sub-areas B-E are unchanged. Footnotes a, b, and e-h are defined in Table 1.

Sub-Area	Outlet	Area (ha)	Width (m)[a]	% Slope[b]	% Imperv	N-Imperv[c]	N-Perv[d]	Subarea Routing[e]	% Routed[f]	HSG[g]	CN[h]
A	RB	0.005	4.97	41.7	100	0.016	---	Outlet	---	---	98
B	F	0.001	1.84	41.7	100	0.016	---	Outlet	---	---	98
C	H	0.005	5.75	41.7	100	0.016	---	Outlet	---	---	98
D	G	0.002	3.96	41.7	100	0.016	---	Outlet	---	---	98
E	G	0.006	11.27	41.7	100	0.016	---	Outlet	---	---	98
F	G	0.00996895	10.40	5.2	40	0.012	0.15	Pervious	85	C	90
G	VS1	0.0086	5.64	9.8	25	0.012	0.15	Outlet	---	C	90
H	RG	0.01364	8.53	6.25	10	0.012	0.15	Pervious	100	D	92
RB	VS1	0.00003105	0.44	0	100	---	---	---	---	---	---
VS1	VS2	0.0014	0.90	6.6	0	---	0.1	---	---	C	90
VS2	RG	0.00146	0.90	5.9	0	---	0.1	---	---	D	92
RG	Out	0.0049	7.30	1	0	---	0.24	---	---	B	85

c. Manning's roughness coefficient of sub-area impervious surface. Sub-areas A-E represent asphalt shingles with an assumed roughness coefficient equal to that of rough asphalt (City of Fayetteville, 2014). Sub-areas F-G represent greenspace. Impervious surfaces consist of smooth concrete. Roughness coefficient acquired from the EPA SWMM (2020) software index. LID sub-areas contain no impervious surface.

d. Manning's roughness coefficient of sub-area pervious surface. Pervious surfaces consist of short, prairie grass, dense brush, and dense grass. Roughness coefficients acquired from EPA SWMM (2020) software index and Drainage Criteria Manual (City of Fayetteville, 2014). Sub-area RB has no surface layer.

The proposed site plan (Figure 7) includes a rain barrel located at the NW corner of the residence to capture discharge exiting the existing downspout. A garden hose will direct rain barrel discharge to the vegetative swale where water will be conveyed 32.2 m east-southeast to a 48.9-m^2 rain garden located on the eastern edge of the property. Though the rain barrel acts as a temporary storage vessel, it is primarily used as a means of intervention. By placing the rain barrel in the proposed location, the discharge exiting the downspout will no longer flow eastward on the existing walkway, underneath the side-porch culvert, and continue down the footpath into the backyard. As the discharge is redirected to the vegetative swale, the footpaths will remain dry, eliminating a safety concern and the inconvenience of puddled rainwater. The discharge is then conveyed to the rain garden where it will infiltrate into the soil, undergo ET, and/or exit the property as runoff.

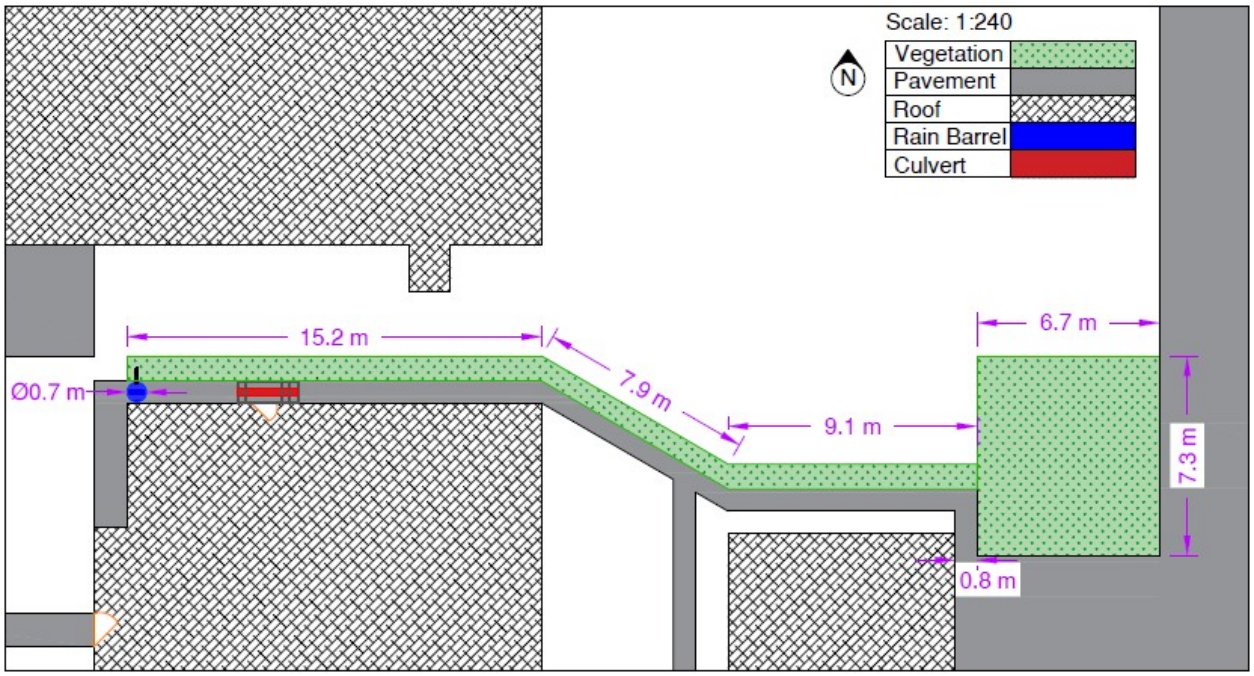

Figure 7. AutoCAD plan view of LID site design at a scale of 1:240 in units of meters. Detailed drawings of LID features are presented in Figures 8, 9, and 10.

The rain barrel characteristics were sourced from a commercially available rain barrel supplied by Gardener's Supply Company (Figure 8). It has a maximum capacity of 284 L (75 gal), stands 0.91 m tall (36 in), and has a maximum diameter of 0.71 m (28 in). There is a 1-in exfiltration valve located 0.1 m (approximately 4 in) from the bottom of the barrel. Runoff enters the barrel through a 0.07-m (2.75-in) pipe at the top of the barrel. Over time, sediment collects at the bottom—this section should be cleaned regularly to avoid drain clogs.

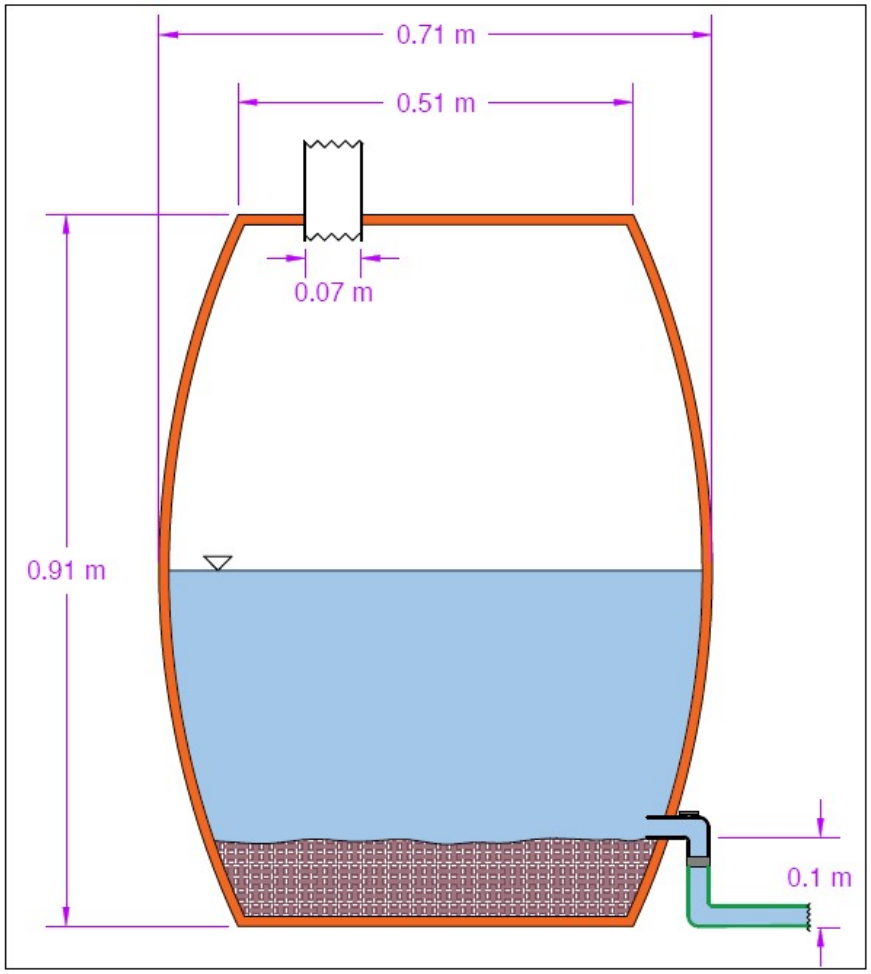

Figure 8. AutoCAD drawing of rain barrel tested in this thesis. Rain barrel has a measured capacity of 234 L (75 gal). Water enters the barrel through a 0.07-m pipe at the top of the barrel and exits through a 1-in exfiltration valve located 0.1 m from the bottom of the barrel. The 4-in sediment collection space at the bottom of the barrel requires regular cleaning to avoid clogging.

The vegetative swales were modeled with identical width and side-slope characteristics (Figure 9). The two swales modeled in this analysis (VS1 and VS2) differ only in total overland flow path length. Each swale has an approximate depth of 0.08 m (3 in) with a 1/1 side-slope. The top-width measures 0.9 m and the bottom-width measures 0.74 m. VS1 has a total length of 15.2 m and VS2 has a total length of 17 m. The total vegetative swale length measures 32.2 m.

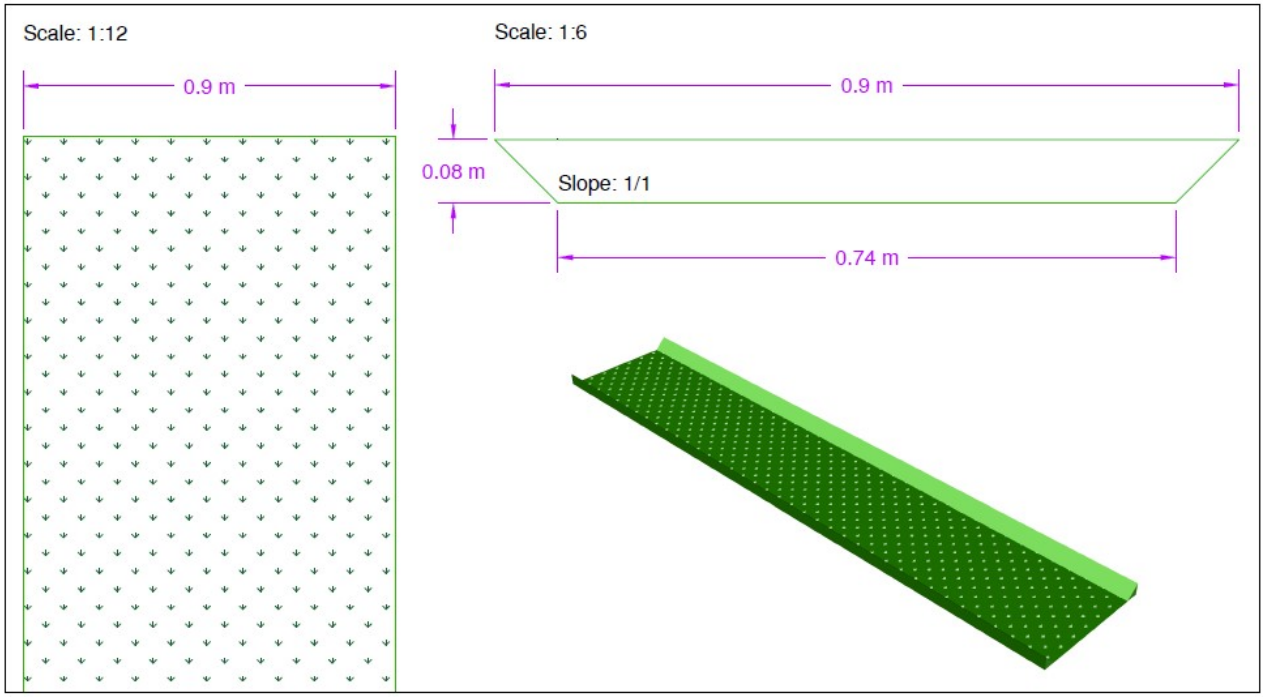

Figure 9. AutoCAD drawing of vegetative swale side-profile and total width. Drawing does not include total swale length (32.2 m).

Three LID scenarios were modeled, each evaluating the change in runoff accompanying a change in rain garden soil thickness. The EPA-suggested depth for rain garden construction ranges from 610 to 1,220 mm (24 to 48 in) (US EPA et al., 2016). Therefore, LID Scenarios A, B, and C model varying soil thicknesses of 610 mm, 915 mm, and 1,220 mm, respectively. These three values were chosen to quantify the impacts of the high-, mid-, and low-points of the suggested range. An artistic rendering of the rain garden for LID Scenario A is depicted in Figure 10.

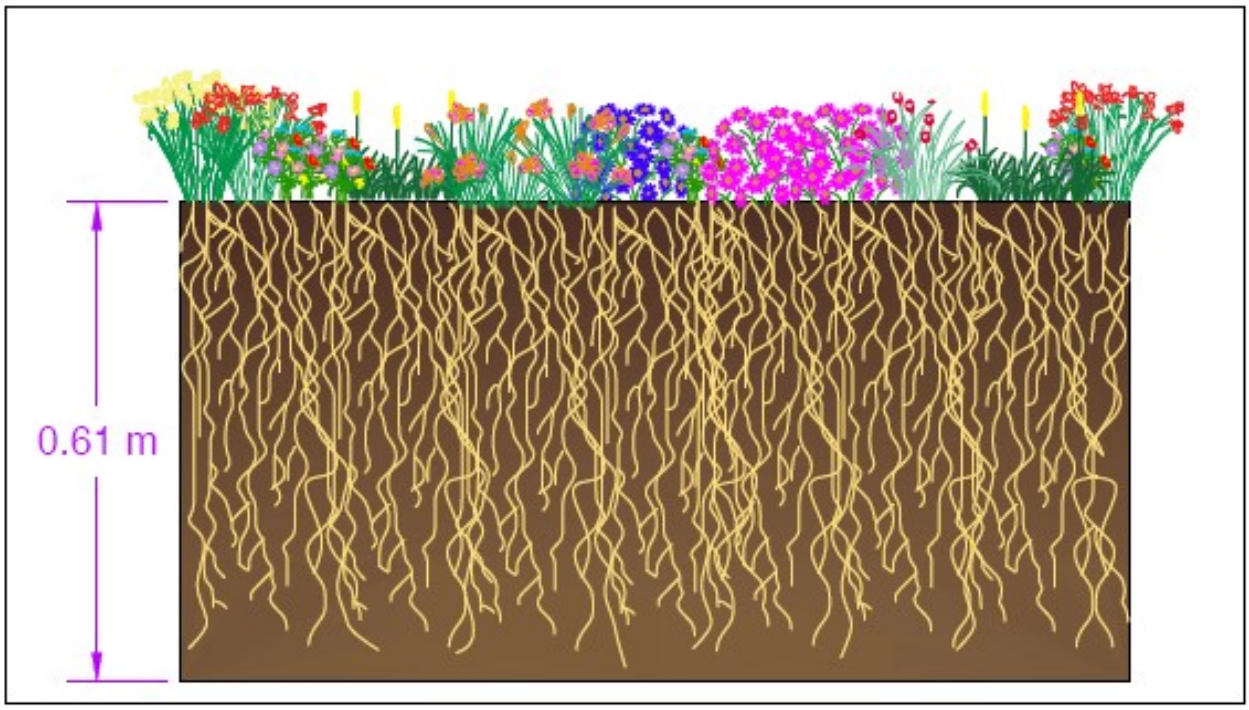

Figure 10. AutoCAD drawing of rain garden side view for LID Scenario A. Soil depth reaches a maximum of 610 mm (DWG Models, 2021). LID Scenarios B and C differ in soil depth: LID Scenario B reaches a maximum depth of 915 mm and LID Scenario C reaches a maximum depth of 1,220 mm. Plants depicted are artist renderings and do not necessarily reflect plants that will be present after construction.

Rain barrel and vegetative swale parameters were constant through each scenario (Table 3; Table 4). In SWMM, rain barrels are modeled as storage layers with 100% void space, an impermeable bottom, and an exfiltration valve (US EPA et al., 2016). The barrel is assumed to be covered and, therefore, receives no precipitation and is not subject to evaporative losses. The flow coefficient and flow exponent parameters were calculated according to US EPA et al. (2016) rain barrel parameter estimates and equations (Appendix C). To prevent flow routing and surface runoff continuity errors in SWMM, the rain barrel was modeled to never overflow—the model is set to allow drainage to occur once internal depth reaches 900 mm, or 98% of capacity.

The rain garden is designed to be highly vegetated with sandy loam soil possessing 55% sand and 15% clay. Conductivity slope is a function of percent sand and clay, equal to 0.48(%sand)+0.85(%clay), which calculates to a conductivity slope of 39.15 (US EPA, 2020). Rain garden berm height was iterated to

determine potential impact, but volumetric reductions were negligible with increased height. Therefore, a 0-mm berm height was chosen to simplify rain garden construction. All other rain garden parameters were chosen in accordance US EPA design recommendations (Table 5) (US EPA et al., 2016; US EPA, 2020).

Table 3. Rain Barrel LID control parameter inputs. Storage potential is a function of barrel height. Drainage is a function of remaining parameters (US EPA et al., 2016; US EPA, 2020).

Parameter	Value	Units
Barrel Height	914.4	mm
Flow Coefficient	14.5	$mm^{0.5}/h$
Flow Exponent	0.5	--
Drain Offset	101.6	mm
Open Level	900	mm

Table 4. Vegetative swale LID control parameter inputs. Parameters are descriptive of swale surface properties (US EPA et al., 2016; US EPA, 2020).

Parameter	Value	Units
Berm Height	80	mm
Vegetation Volume	80%	--
Roughness (n)	0.1	--
Side Slope (run/rise)	1/1	--
Width	90	mm

Table 5. Rain Garden LID control parameter inputs. Parameters "Berm Height" through "Slope" are descriptive of surface properties. Storage potential is a function of remaining parameters (US EPA et al., 2016; US EPA, 2020).

Parameter	Value	Units
Berm Height	0	mm
Vegetation Volume	80%	--
Roughness	0.24	--
Slope	1%	--
Soil Thickness		
Scenario A	610	mm
Scenario B	915	mm
Scenario C	1,220	mm
Porosity	0.45	--
Field Capacity	0.15	--
Wilting Point	0.05	--
Conductivity	76.2	mm/h
Conductivity Slope	39.15	--
Suction Head	51	mm
Initially Saturated	15%	--

Shannon-Weiner Diversity Index

A diversity index was performed to determine species richness (S), evenness (E) and overall biodiversity (H) of the 48.9-m^2 area where the rain garden will be located. Existing flowering species were categorized and counted. To determine the potential biodiversity of this area, it is assumed that two separate wildflower seed mixes will be evenly broadcast over the site. To ensure the presence of pollinator-preferred flowers, two pollinator-specific wildflower mixes are considered (Eden Brothers, 2021a, 2021b).To estimate potential changes in biodiversity, species sample numbers were randomized using Excel's "random between" function with a range of 0 to 10. A maximum of 10 samples of each species was utilized to demonstrate the method for measuring an increase in biodiversity without grossly overestimating the potential for change. The inclusion of this methodology is purely qualitative to

demonstrate potential changes in biodiversity for this particular design. During implementation, homeowners have the freedom to choose any number of flowering plants (including none), so index calculations presented in this thesis do not represent a tested or recommended scenario.

Results

Soil Analysis

Most soil on the property contains high quantities of clay (Table 6), solidifying the need to import a more suitable soil for rain garden development. As soils high in clay allow very slow infiltration and have high runoff potential, constructing a rain garden with these naturally occurring soils would prove unsuccessful in its ability to reduce discharge.

Table 6. Experimentally determined properties of collected soil samples. Samples A through I were collected from the backyard and side yard of the residence while samples J through L were collected from the front yard of the residence. Low bulk density values indicate presence of high quantities of soil organic matter (Brown and Wherrett, 2014).

Sample	%Sand	%Silt	%Clay	Texture	θ_g (g/g)	ρ_b (g/cm^3)	θ_v (g/g)	Porosity
A	42.5	12.1	45.4	Clay	0.18	0.80	0.14	70%
B	44.5	10.5	44.9	Clay	0.18	1.02	0.18	61%
C	39.7	10.1	50.3	Clay	0.20	0.84	0.17	68%
D	40.5	11.1	48.4	Clay	0.20	1.33	0.27	50%
E	37.6	12.4	50.0	Clay	0.20	1.18	0.24	55%
F	36.6	13.0	50.4	Clay	0.20	1.19	0.24	55%
G	44.9	10.6	44.5	Clay	0.22	1.02	0.23	61%
H	41.5	9.8	48.7	Clay	0.20	1.00	0.20	62%
I	39.8	10.1	50.1	Clay	0.20	0.91	0.18	66%
J	44.2	21.0	34.8	Clay Loam	0.28	0.81	0.23	69%
K	53.1	16.5	30.4	Sandy Clay Loam	0.22	1.12	0.25	58%
L	47.9	12.2	40.0	Sandy Clay	0.20	1.22	0.24	54%

SWMM Analysis

Base Scenario

The model results show 0% surface runoff and flow routing continuity errors, suggesting successful parameter estimates for all sub-areas. For the base scenario, onset of discharge begins at the 1-h time-step and reaches its peak at the 10-h time-step for all design storms (Figure 11). Runoff fully attenuates for the 25-yr event at the 30-h time-step while the 10-yr, 5-yr, 2-yr, and 1-yr events fully attenuate at the

29.5-h time-step. Peak discharge and total volumetric discharge for each 24-h storm are summarized in Table 7.

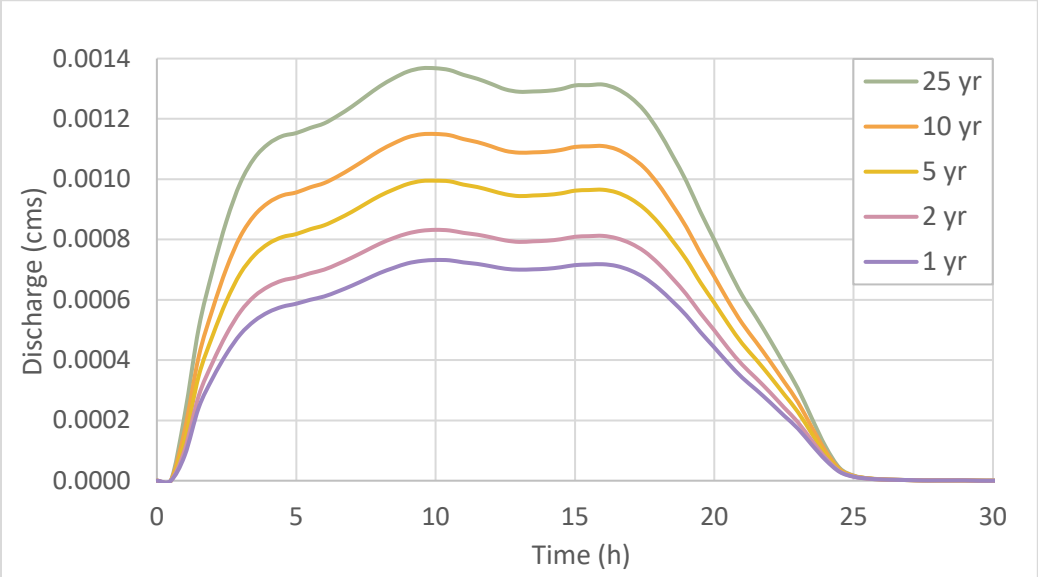

Figure 11. Base scenario hydrographs for 24-h storms. Discharge values represent present-day land use outflow characteristics. Cumulative precipitation depths total 159 mm, 135 mm, 118 mm, 100 mm, and 89 mm, respectively (NOAA, 2021).

Table 7. Base scenario summary comparison of total sub-area outflow characteristics for 24-h storms.

Parameter of Interest	25-yr	10-yr	5-yr	2-yr	1-yr
Discharge Onset (h)	1	1	1	1	1
Peak Discharge (CMS)	0.0014	0.0012	0.0010	0.0008	0.0007
Total Volumetric Discharge (m^3)	87.26	73.23	63.31	52.86	46.51
Time of Attenuation (h)	30	29.5	29.5	29.5	29.5

LID Scenarios

In LID Scenario A, there is a delay in discharge onset for each 24-h storm (Figure 12). We also see a slight decrease in peak discharge rates, though the percent-change is negligible (< 1%). However, the delay in discharge onset causes a substantial reduction in total volumetric outflow. The greatest reduction is seen with the 1-yr storm at 21.2% while the 25-yr storm shows a 12.3% reduction in total volumetric outflow. Outflow characteristics, including peak discharge rates, total volumetric discharge, and time of attenuation are summarized in Table 8.

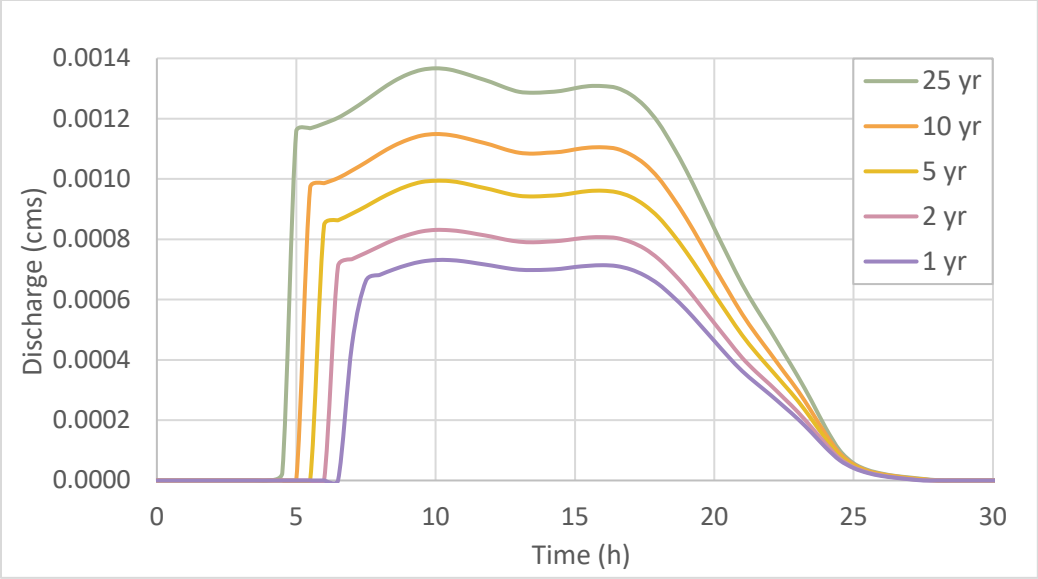

Figure 12. LID Scenario A hydrographs, 24-h storms. Discharge values represent designed LID network, including one rain barrel (284 L), two vegetative swales (total length, 32.2 m), and one 48.9-m^2 rain garden with a soil depth of 610 mm. Cumulative precipitation depths total 159 mm, 135 mm, 118 mm, 100 mm, and 89 mm, respectively (NOAA, 2021).

Table 8. LID Scenario A summary comparison of total sub-area outflow characteristics for 24-h storms.

Parameter of Interest	25-yr	10-yr	5-yr	2-yr	1-yr
Discharge Onset (h)	4.5	5.5	6	6.5	7
Peak Discharge (CMS)	0.0014	0.0012	0.0010	0.0008	0.0007
Total Volumetric Discharge (m^3)	76.50	62.69	52.92	43.13	36.63
Percent Reduction[a]	12.3%	14.4%	16.4%	18.4%	21.2%
Time of Attenuation (h)	28.5	28	28	28	27.5

a. Compared with base scenario.

There are greater reductions in total volumetric discharge for LID Scenarios B and C. The 305-mm increase in soil depth (from LID Scenario A to B) causes further delays in discharge onset (Figure 13). These delays become less pronounced as total precipitation increases (Table 9). When compared with the base scenario, the greatest reduction is seen with the 1-yr storm at 33.5% while the 25-yr storm shows a 16.9% reduction in total volumetric outflow. When soil depth is increased to the maximum recommended depth of 1,220 mm, the greatest delays in discharge onset (Figure 14) and reductions in total volumetric discharge occur (Table 10). Following the established trend, the greatest volumetric reduction is seen with the 1-yr storm at 42.6% while the 25-yr storm shows a 23.6% reduction.

Discharge onset for the 25-yr storm event remains constant through each LID scenario at the 4.5-h time-step indicating a systematic inability to attenuate discharge, as successfully, for more infrequent, highly intense storm events. Once rain garden saturation is met, discharge onset begins. Despite this, LID Scenario B experiences a reduction in discharge magnitude from the 4.5- to 5.5-h time-steps while LID Scenario C experiences this reduction from the 4.5- to 7-h time-steps when compared to LID Scenario A. This can be explained by the reduction in relative intensity, and subsequent reduction in total overland flow, of the model storm event between the 3.5- and 5.5-h time-steps. There is not enough available pore space to eliminate runoff during these time-steps for either scenario, but the tested systems demonstrate an ability to reduce the incremental magnitudes.

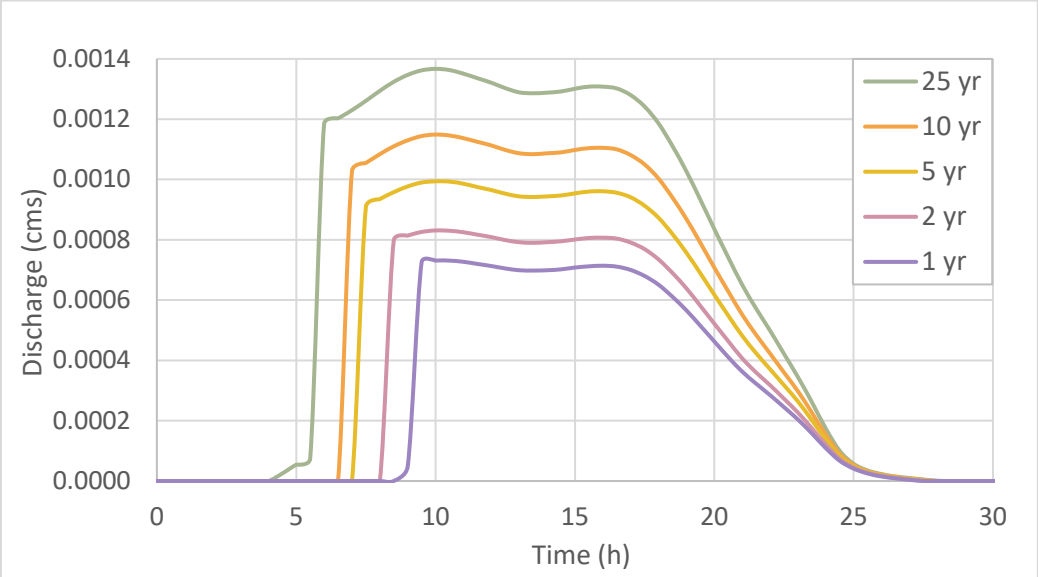

Figure 13. LID Scenario B hydrographs, 24-h storms. Discharge values represent designed LID network, including one rain barrel (284 L), two vegetative swales (total length, 32.2 m), and one 48.9-m^2 rain garden with a soil depth of 915 mm. Cumulative precipitation depths total 159 mm, 135 mm, 118 mm, 100 mm, and 89 mm, respectively (NOAA, 2021).

Table 9. LID Scenario B summary comparison of total sub-area outflow characteristics for 24-h storms.

Parameter of Interest	25-yr	10-yr	5-yr	2-yr	1-yr
Discharge Onset (h)	4.5	7	7.5	8.5	9
Peak Discharge (CMS)	0.0014	0.0012	0.0010	0.0008	0.0007
Total Volumetric Discharge (m^3)	72.54	57.36	48.25	37.77	30.94
Percent Reduction[a]	16.9%	21.7%	23.8%	28.5%	33.5%
Time of Attenuation (h)	28.5	28	28	28	27.5

a. Compared with base scenario.

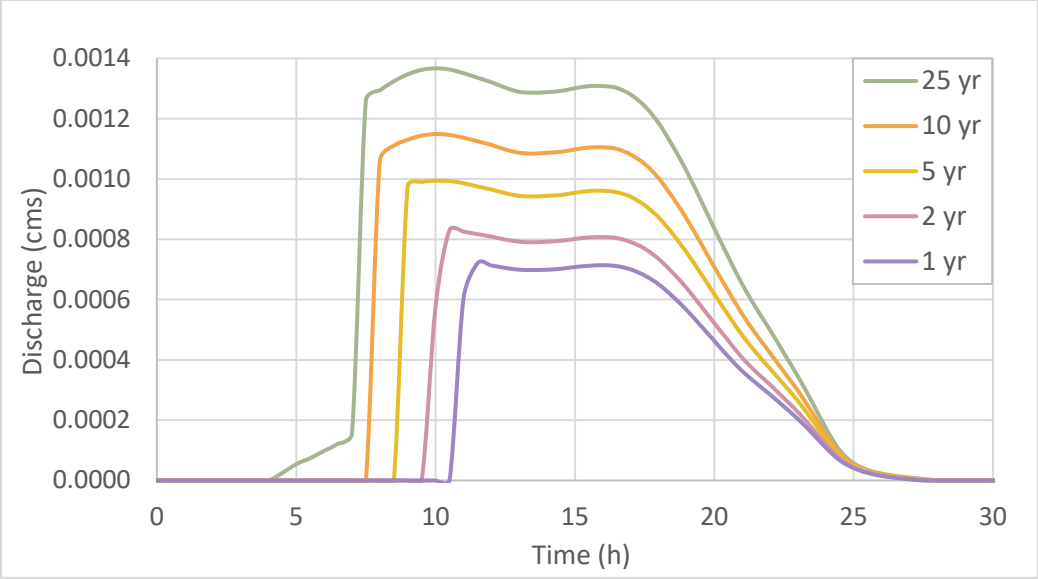

Figure 14. LID Scenario C hydrographs, 24-h storms. Discharge values represent designed LID network, including one rain barrel (284 L), two vegetative swales (total length, 32.2 m), and one 48.9-m^2 rain garden with a soil depth of 1,220 mm. Cumulative precipitation depths total 159 mm, 135 mm, 118 mm, 100 mm, and 89 mm, respectively (NOAA, 2021).

Table 10. LID Scenario C summary comparison of total sub-area outflow characteristics for 24-h storms.

Parameter of Interest	25-yr	10-yr	5-yr	2-yr	1-yr
Discharge Onset (h)	4.5	8	9	10	11
Peak Discharge (CMS)	0.0014	0.0012	0.0010	0.0008	0.0007
Total Volumetric Discharge (m^3)	66.71	53.56	43.20	32.93	26.69
Percent Reduction[a]	23.6%	26.9%	31.8%	37.7%	42.6%
Time of Attenuation (h)	28.5	28	28	28	27.5

a. Compared with base scenario.

Diversity Index Analysis

In the existing area of interest, five flowering plants were discovered, including purple and white Anemone blanda, Tradescantia virginiana, Taraxacum officinale, and Vinca major. A total of 132 samples were tallied. With an S value of 5, the maximum possible diversity (H_{max}) calculates to 1.609 while the actual diversity (H) calculates to 1.116. Therefore, the existing evenness of flowering species across the habitat is 0.693. For the proposed wildflower planting method, the S value increases to 27 (440% increase), H_{max} calculates to 3.296, and H calculates to 2.753 (147% increase). These values indicate an evenness of potential flowering species across the habitat of 0.835 (20.5% increase). A list of unique species, sample numbers, calculations, and index equations are available in Appendix D.

Discussion and Future Opportunities

For each 24-h design storm, there is a notable reduction in total volumetric discharge demonstrated by each LID Scenario. Though peak discharge decreases, these values represent a less than 1% change for each scenario, rendering these reductions negligible. The most prominent reduction in volumetric discharge is generated by the deepest rain garden soil profile (LID Scenario C) as this scenario offers the greatest available pore space to fill with incoming stormwater runoff (Figure 15).

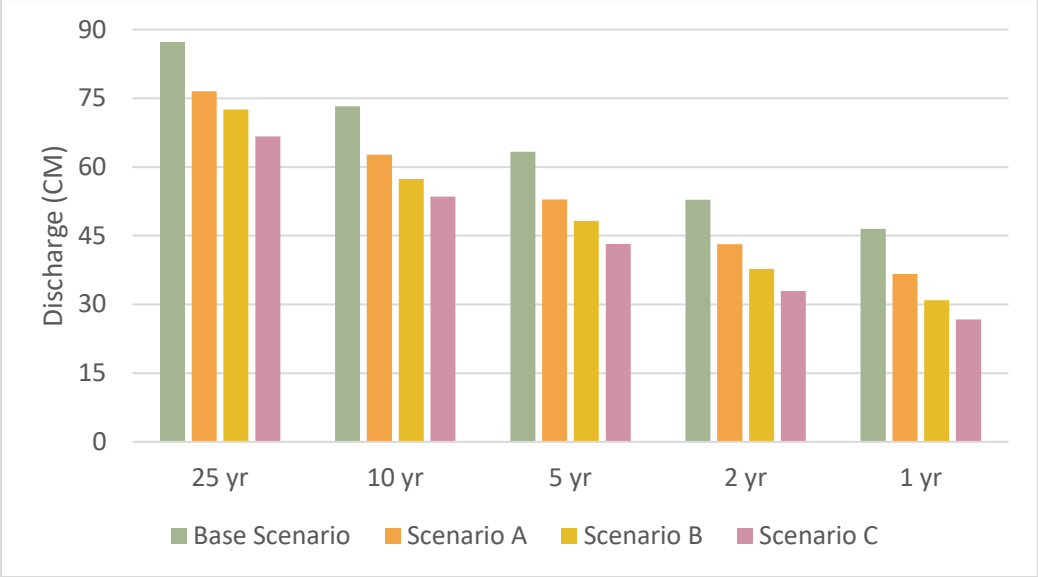

Figure 15. Graphical comparison of total volumetric discharge for all modeled scenarios. Base Scenario represents present-day land-use conditions. Scenarios A, B, and C differ only in rain garden soil depth, measured at 610, 915, and 1,220 mm, respectively. Cumulative precipitation depths total 159 mm, 135 mm, 118 mm, 100 mm, and 89 mm, respectively (NOAA, 2021).

When assessing the rain garden LID sub-area as a standalone feature, we can evaluate the total runoff exiting the sub-area versus the soil depth for each scenario. As rain garden soil depth (mm) increases, available pore space increases and total rain garden runoff (mm) decreases. The model generates an equation relating these two metrics. With this relationship, total runoff from this rain garden at any proposed soil depth can be calculated:

$$R = -0.34D + (11.86P - 108) \quad \text{Eq. 1}$$

where R = rain garden runoff in mm

D = rain garden soil depth in mm

P = total precipitation in mm

This reduction in runoff is attributed to the increased storage potential that accompanies increased available pore space. The slope, -0.34, adjusts for this storage potential and is a function of model parameters set by the user, including porosity, field capacity, wilting point, and initial saturation. If any of these values are changed, the slope will also change. An engineer or LID professional can apply Eq. 1 to determine whether a proposed rain garden soil depth (and subsequently, available pore space) will adequately control stormwater runoff. Alternatively, Eq. 1 can be rearranged to calculate the necessary soil depth to meet a particular runoff target. Example calculations for runoff prediction can be found in Appendix E.

This reduction in discharge does not necessarily indicate that the deepest soil profile is the best choice for every homeowner. With each increase in soil depth, cost appreciably increases, as well. The soil is the most expensive element of the design, costing a minimum of $3,580 (at the time of writing) to fill the excavated area to a depth of 610 mm (Table 11). To fully implement LID Scenario A, assuming the homeowner rented all necessary equipment and performed the work themselves, cost would reach an estimated $4,399. Under the same assumptions, LID Scenario B would cost a total of $6,099 and LID Scenario C would cost a total of $7,889. Cost per unit volume discharge avoided, averaged across all storms, with each LID scenario calculates to $0.33/L ($1.23/gal), $0.31/L ($1.16/gal), and $0.28/L ($1.07/gal) respectively (Figure 16). Should a homeowner decide to implement one of the proposed scenarios, the differences in capital cost and average cost per unit volume runoff avoided between each design will likely weigh heavily in their decision-making process.

Table 11. Capital cost breakdown of LID Scenarios. Soil volume is the only changing parameter between each scenario.

Item	Cost/Item	Quantity	Cost	Source
Deluxe Rain Barrel, 75 gal	$179	1	$179	Gardener's Supply Company
Garden hose, 6 ft	$13	1	$13	Lowes
Soil, yd^3	$89.50			
Scenario A – 610 mm		40	$3,580	Lyngso Garden
Scenario B – 915 mm		59	$5,281	
Scenario C – 1,220 mm		79	$7,071	
Seed Mix, All Perennial	$12.95	1	$12.95	Eden Brothers, Wildflower Seed Mix
Seed Mix, Late Bloomers	$12.95	1	$12.95	Eden Brothers, Fall Blooming Seed Mix
Zoysiagrass, Seed & Mulch	$45.99	1	$45.99	Scotts
Trencher Rental, 1 day	$215	1	$215	Sunbelt Rentals, 24" Track Trencher
Excavator Rental, 1 day	$340	1	$340	Sunbelt Rentals, 6000-lb Mini

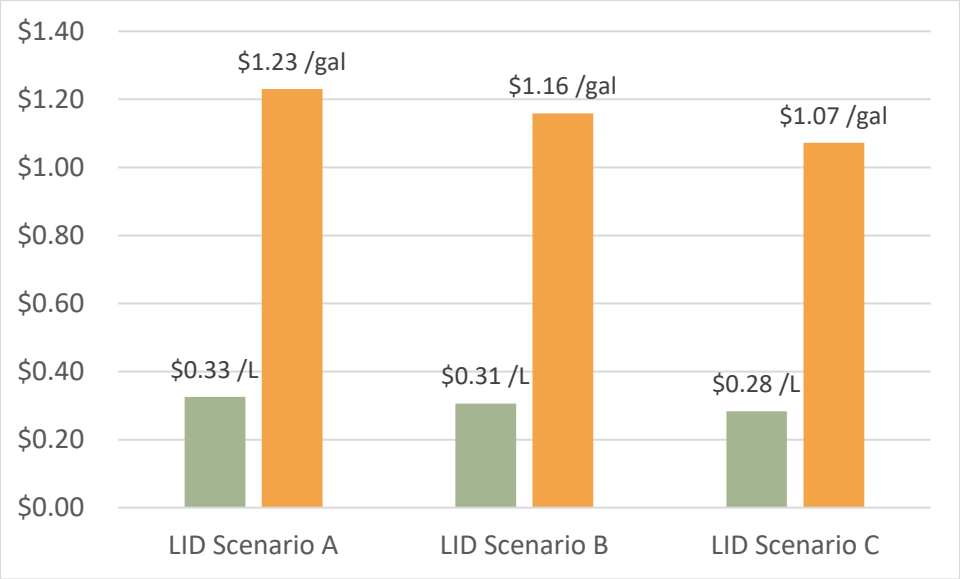

Figure 16. Cost per unit volume discharge avoided, averaged across all storms, for each LID design scenario when compared to the base scenario. Capital cost for LID Scenario A total $4,399, LID Scenario B totals $6,099, and LID Scenario C totals $7,889.

Landscaping does provide economic value to a property, ranging from an increase of 5.5% to 12.7% (Dietz, 2013). However, no matter the scenario a homeowner chooses to implement, the value of their home would increase an equal amount due to the nature of the designs. The only changing element is the soil depth of the rain garden, each of which provide equal aesthetic value. Therefore, a homeowner would

gain the most economic benefit by implementing LID Scenario A as it requires the lowest initial investment ($4,399).

The property used in this study (524 N Storer Ave, Fayetteville, AR 72701) has an estimated worth of $256,000 in April 2021 (realtor.com, 2021). If the homeowner implemented LID Scenario A at the time of writing, spent $100 per year on maintenance for 10 years, and chose to sell the property 10 years after LID construction, assuming a 6% increase in value due to landscaping, the home would increase in value by $15,360 more than during the same time period if the homeowner chosen not to invest in landscaping. Assuming an annual interest of 4%, this calculates to a net present value (NPV) of $5,167. Applying the same logic to LID Scenarios B and C, NPV calculates to $3,467 and $1,677. Therefore, it is recommended to opt for a rain garden soil depth of 610 mm (LID Scenario A). This scenario provides adequate runoff reduction, requires the lowest initial investment, and yields the highest NPV.

Conclusion

The addition of LID technologies, specifically those with an ability to store water and promote infiltration, can provide environmental and economic benefit, even if the LID sub-area is relatively small. Residential LID designs can be engineered to resolve issues surrounding erosion, flooding or puddling, washout, and other issues related to stormwater runoff. In general, when designing a rain garden, available pore space will play a crucial role in the mitigation of volumetric discharge. This study has demonstrated an ability to reduce discharge from 12-42% with the addition of one rain barrel, two vegetative swales, and one 48.9-m^2 rain garden. The combination of these four LID structures calculate to 13.2% the size of the total drainage service area, confirming the positive impact of small-scale designs. The greatest reductions are seen with the most frequent storm events and the deepest rain garden soil profile (highest available pore space). However, as importing soil is often the most expensive aspect of rain garden implementation, designing the deepest possible rain garden is not always to best choice for homeowners. When choosing LID designs, homeowners must consider the financial commitment they are

willing to make and how the implementation of each element will affect the value of their home. As maintenance is a common deterrent in LID adoption, homeowners are encouraged to opt for low-maintenance designs—incorporating native flora provides this benefit in addition to its ability to improve relative biodiversity.

Acknowledgements

I would like to sincerely thank my advisor, Dr. Benjamin Runkle, for his unending support, encouragement, and words of wisdom throughout the tenure of this study. Without his guidance, I would be nowhere. I am eternally grateful to Dr. Kieu Ngoc Le for guiding me in the topic selection and problem definition of this project, as well as always pushing me to be the very best version of myself I can muster. I would also like to thank my committee members, Dr. Brian Haggard and Dr. David Miller, for aiding me in the completion of this thesis. Lastly, I would like to thank my fiancé, Christian Maas, for his unwavering support, love, and understanding. We can finally go out on Friday nights again.

References

Abi Aad, M. P., Suidan, M. T., Shuster, W. D. (2010). Modeling techniques of best management practices: Rain barrels and rain gardens using EPA SWMM-5. *Journal of Hydrologic Engineering*, *15*(6), 434–443. https://doi.org/10.1061/(ASCE)HE.1943-5584.0000136

Adamson, N. L., Borders, B., Cruz, J. K., Foltz Jordan, S., Gill, K., Hopwood, J., … Vaughan, M. (2017). Pollinator plants: Southern Plains region (Version 03). Xerces Society for Invertebrate Conservation. Retrieved from https://xerces.org/publications/plant-lists/pollinator-plants-southern-plains-region

AGFC. (2021). Native gardening for Arkansas pollinators. Retrieved January 29, 2021, from https://www.agfc.com/en/wildlife-management/awap/monarch-pollinator-conservation/

Arkansas GIS Office. (2020). *County boundaries of Arkansas* [Vector digital data]. Retrieved from https://gis.arkansas.gov/product/county-boundary-polygons/

Backus, B. (2020, July 30). Soil hydrometer testing: Sedimentation method techniques & equipment. Retrieved April 17, 2021, from https://www.globalgilson.com/blog/soil-hydrometer-analysis

Brown, K., Wherrett, A. (2014). Bulk density: Measurement. Retrieved March 28, 2021, from http://soilquality.org.au/factsheets/bulk-density-measurement

Buchhorn, S. (2018). *Rainwater harvesting in Champaign-Urbana: A study on the summer 2017 rain barrel sale*. Urbana-Champaign, IL. Retrieved from https://www.ideals.illinois.edu/handle/2142/103929

City of Fayetteville. (2014, July 1). Drainage criteria manual. City of Fayetteville. Retrieved from https://www.fayetteville-ar.gov/DocumentCenter/View/2248/Drainage-Criteria-Manual-2014-PDF

City of Fayetteville. (2021). *General reference and data downloads* [Vector digital downloads]. Fayetteville, AR. Retrieved from https://maps.fayetteville-ar.gov/viewer/index.html?webmap=46ac3a6201624738a961f1f3123d7d5b

Coleman, S., Hurley, S., Rizzo, D., Koliba, C., Zia, A. (2018). From the household to watershed: A cross-scale analysis of residential intention to adopt green stormwater infrastructure. *Landscape & Urban Planning*, *180*, 195–206. https://doi.org/10.1016/j.landurbplan.2018.09.005

DelVecchio, T., Welker, A., Wadzuk, B. M. (2020). Exploration of volume reduction via infiltration and evapotranspiration for different soil types in rain garden lysimeters. *Journal of Sustainable Water in the Built Environment*, *6*(1), 04019008. https://doi.org/10.1061/JSWBAY.0000894

Dietz, D. (2013, June 26). Does landscaping increase property value? [Blog]. Retrieved April 1, 2021, from https://www.parealtors.org/does-landscaping-increase-property-value/

DWG Models. (2021). *Flowers* [CAD Drawings]. Retrieved from https://dwgmodels.com/668-flowers.html

Earth Science Information Center. (2013). *High resolution: National hydrography dataset flowline feature* [Vector downloadable data]. Earth Science Information Center. Retrieved from http://gis.arkansas.gov/product/high-resolution-national-hydrography-dataset-flowline-feature-line/

Earth Science Information Center. (2019). *Medium resolution: National hydrography dataset flowline feature* [Vector downloadable data]. Earth Science Information Center. Retrieved from http://gis.arkansas.gov/product/medium-resolution-national-hydrography-dataset-flowline-feature-line/

Eden Brothers. (2021a). Bird & butterfly wildflower seed mix. Retrieved April 21, 2021, from https://www.edenbrothers.com/store/bb_wildflower_seed_mix.html

Eden Brothers. (2021b). The Bee's Knees pollinator wildflower seed mix. Retrieved April 21, 2021, from https://www.edenbrothers.com/store/pollinator-wildflower-seed-mix.html

Flynn, K. M., Traver, R. G. (2013). Green infrastructure life cycle assessment: A bio-infiltration case study. *Ecological Engineering*, *55*, 9–22. https://doi.org/10.1016/j.ecoleng.2013.01.004

Google Earth. (2021). Map showing location of 524 N Storer Ave, Fayetteville, AR 72701. Google. Retrieved from https://earth.google.com/web/

Hess, A., Wadzuk, B., Welker, A. (2017). Evapotranspiration in rain gardens using weighing lysimeters. *Journal of Irrigation & Drainage Engineering*, *143*(6), 04017004. https://doi.org/10.1061/(ASCE)IR.1943-4774.0001157

Ismail, A., Sapari, N., Abdul Wahab, M. (2014). Vegetative swale for treatment of stormwater runoff from construction site. *Pertanika J. Sci. Technol*, *22*(1), 55–64.

Jennings, A. A., Adeel, A. A., Hopkins, A., Litofsky, A. L., Wellstead, S. W. (2013). Rain barrel–Urban garden stormwater management performance. *Journal of Environmental Engineering*, *139*(5), 757–765. https://doi.org/10.1061/(ASCE)EE.1943-7870.0000663

Jennings, A. A., Berger, M. A., Hale, J. D. (2015). Hydraulic and hydrologic performance of residential rain gardens. *Journal of Environmental Engineering (U.S.), 141*(11). https://doi.org/10.1061/(ASCE)EE.1943-7870.0000967

Kral-O'Brien, K. C., O'Brien, P. L., Hovick, T. J., Harmon, J. P. (2021). Meta-analysis: Higher plant richness supports higher pollinator richness across many land use types. *Annals of the Entomological Society of America*, *114*(2), 267–275. https://doi.org/10.1093/aesa/saaa061

Liu, L., Zhu, K., Wurzburger, N., Zhang, J. (2020). Relationships between plant diversity and soil microbial diversity vary across taxonomic groups and spatial scales. *Ecosphere*, *11*(1), 20. https://doi.org/10.1002/ecs2.2999

Mohammed, W., Welker, A. L., Press, J. (2019). Effect of geotechnical parameters on the percolation performance of an established rain garden in Pennsylvania. In *Geo-Congress 2019: Geotechnical Materials, Modeling, & Testing* (pp. 733–742). Philadelphia, PA, United states: American Society of Civil Engineers. https://doi.org/10.1061/9780784482124.074

NOAA. (2021). NOAA atlas 14-point precipitation frequency estimates: AR. Retrieved February 9, 2021, from https://hdsc.nws.noaa.gov/hdsc/pfds/pfds_map_cont.html?bkmrk=ar

Peng, Z., Jinyan, K., Wenbin, P., Xin, Z., Yuanbin, C. (2019). Effects of low-impact development on urban rainfall runoff under different rainfall characteristics. *Polish Journal of Environmental Studies*, *28*(2), 771–783. https://doi.org/10.15244/pjoes/85348

realtor.com. (2021). 524 N Storer Ave, Fayetteville, AR 72701. Retrieved April 1, 2021, from https://www.realtor.com/myhome/524-N-Storer-Ave_Fayetteville_AR_72701_M86321-40584/homevalue

Ross, C. W., Prihodko, L., Anchang, J., Kumar, S., Ji, W., Hanan, N. P. (2018). Global hydrologic soil groups (HYSOGs250m) for curve number-based runoff modeling. Oak Ridge, Tennessee, USA: ORNL DAAC. https://doi.org/10.3334/ORNLDAAC/1566

Stroud Water Research Center. (2020). Model my watershed (Version 1.27) [Software]. Stroud Water Research Center. Retrieved from https://wikiwatershed.org/

US EPA. (2020). Storm water management model (Version 5.1.015) [Software]. Cincinnati, Ohio: Centers for Environmental Solutions & Emergency Response. Retrieved from www.epa.gov/swmm

US EPA, Gironas, J., Roesner, L. A., Davis, J. (2009, July). Storm water management model application manual. US EPA. Retrieved from https://www.epa.gov/water-research/storm-water-management-model-swmm

US EPA, Rossman, L. A., Huber, W. C. (2016, July). Storm water management model reference manual: Volume III - water quality. US EPA. Retrieved from https://www.epa.gov/water-research/storm-water-management-model-swmm

USDA-NRCS, USGS, EPA. (2015). *National watershed boundary dataset* [Vector downloadable data]. Retrieved from http://gis.arkansas.gov/product/12-digit-watershed-boundary-dataset-polygon/

USGS. (2020). *USGS onemeter x39y400 AR R6-WashingtonCO 2015* [Raster downloadable data]. USGS. Retrieved from https://www.sciencebase.gov/catalog/item/5eaa4b7382cefae35a21f717

Wadzuk, B. M., Hickman, J. M., Traver, R. G. (2015). Understanding the role of evapotranspiration in bioretention: Mesocosm study. *Journal of Sustainable Water in the Built Environment*, *1*(2), 04014002. https://doi.org/10.1061/JSWBAY.0000794

Werner, J., Woodward, D. E., Nielsen, R., Dobos, R., Hjelmfelt, A. (2007). Chapter 7: Hydrologic soil gorups. In *National Engineering Handbook (NEH) Part 630, Hydrology*. USDA-NRCS. Retrieved from https://directives.sc.egov.usda.gov/OpenNonWebContent.aspx?content=17757.wba

Appendix A. Wildflower Species Native to NW Arkansas and the Southern Plains Region

It is generally best to incorporate a mix of species that bloom during different times of the year to ensure a lengthy blooming season while early- and late-blooming flowers are of particular importance to the health of native pollinators (AGFC, 2021). Wildflower species native to this region are presented in Table A-1.

Table A-1. A non-exhaustive list of wildflower species native to Northwest Arkansas and the Southeast Plains Region of the U.S. organized by blooming season (Adamson et al., 2017; AGFC, 2021).

Season	Common Name	Scientific Name	Flower Color	Max Height	Water Needs[a]
Spring	Prairie spiderwort	Tradescantia occidentalis	blue	600 mm	L
	Eastern beebalm	Monarda bradburiana	pink/white	600 mm	L/M
	Golden alexanders	Zizia aurea	gold	760 mm	L/M
	Wild bergamot	Monarda fistulosa	pink/purple	1.2 m	M
Spring – Summer	Antelopehorn milkweed	Asclepiasis viridis	green/purple	600 mm	M
	Scarlet globemallow	Sphaeralcea coccinea	orange	300 mm	L
	Butterfly milkweed	Asclepias tuberosa	orange	760 mm	L/M
	Rose vervain	Glandularia canadensis	pink	450 mm	L
	Lanceleaf coreopsis	Coreopsis lanceolata	yellow	900 mm	L
Summer	Pale purple coneflower	Echinacea purpurea	purple	1.2 m	L/M
	Lemon beebalm	Monarda citriodora	purple	600 mm	L
	White prairie clover	Dalea candida	white	600 mm	L
	Black-eyed Susan	Rudbeckia fulgida	yellow	900 mm	L/M
	Mexican hat	Ratibida columnifera	yellow/red	600 mm	L
Summer – Fall	Clustered mountain mint	Pycnantheum muticum	white	900 mm	L/M
	Purple prairie clover	Dalea purpurea	lavender	900 mm	L
	Downy ragged goldenrod	Solidago petiolaris	yellow	1.2 m	L/M
	Dotted blazing star	Liatris punctata	purple	760 mm	M
Fall	Aromatic aster	Symphyotrichum oblongifolium	purple	600 mm	L
	Giant goldenrod	Solidago gigantea	yellow	2.1 m	M
	Maximilian sunflower	Helianthus maximiliani	yellow	2.4 m	L
	New England aster	Symphyotrichum novea-angliae	purple	1.8 m	M
	Azure blue sage	Salvia azurea	blue	1.5 m	L/M

[a] L – low water needs, M – medium water needs

Appendix B. 3D Google Earth Images of Location of Interest

Three-dimensional top-view images of the location of interest are depicted in Figures B-1 and B-2.

Figure B-1. 3D image of 2-block radius of 524 N Storer Ave, Fayetteville, AR 72701 (Google Earth, 2021).

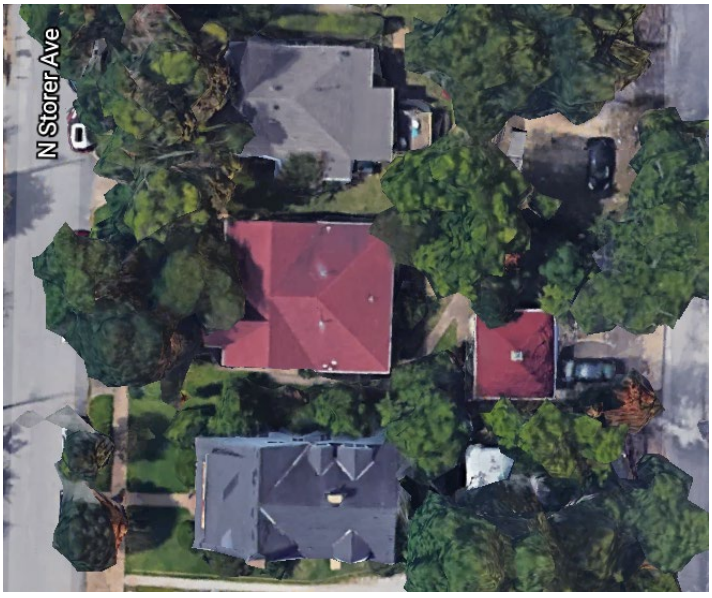

Figure B-2. Close-up 3D image of 524 N Storer Ave, Fayetteville, AR 72701 (Google Earth, 2021).

Appendix C. Rain Barrel Exfiltration

Due to the complex nature of underdrain hydraulics, SWMM uses an empirical power law to model underdrain outflow, $q_3 = C_{3D}(h_3)^{\eta_{3D}}$ (US EPA et al., 2016). C_{3D} represents the underdrain discharge coefficient, h_3 represents hydraulic head, and η_{3D} represents the underdrain discharge exponent. If $\eta_{3D} = 0.5$, then q_3 is equivalent to the standard orifice equation, $q = C_d A\sqrt{2gh}$. Then, $C_{3D} = 0.6\left(\frac{A_1}{A_2}\right)\sqrt{2g}$, where A_1 is the barrel surface area and A_2 is the area of the drain valve opening. Equivalently, $C_{3D} = 4.8\left(\frac{D_{drain}}{D_{barrel}}\right)^2$ where D_{drain} and D_{barrel} are equal to the drain diameter and barrel diameter, respectively, with units of $ft^{0.5}/sec$. A conversion factor is necessary as SWMM uses input units of $mm^{0.5}/h$. Therefore, the final drain coefficient equation becomes $C_{3D} = 4.8\left(\frac{D_{drain}}{D_{barrel}}\right)^2 * 62{,}768$.

The rain barrel used in this study has a 1-in drain diameter and a 28-in barrel diameter. To attenuate exfiltration, the drain diameter is modeled as partially closed, reducing the value of D_{drain} by approximately 80%. This indicates the drain valve is open to about one-fifth its total capacity. The flow coefficient equation becomes $C_{3D} = 4.8\left(\frac{0.194}{28}\right)^2 * 62{,}768$. This equates to the input parameter of $14.5\ mm^{0.5}/h$.

Appendix D. Shannon-Weiner Diversity Index

Species name, plant quantities, and calculations are presented in Table D-1. Calculations follow below.

Table D-1. Shannon-Weiner Diversity Index calculation table.

Species	Plant Quantities	pi	$\ln pi$	$pi * \ln pi$
Base Scenario				
Anemone blanda, purple	8	0.061	-2.803	-0.170
Anemone blanda, white	1	0.008	-4.883	-0.037
Tradescantia virginiana	39	0.295	-1.219	-0.360
Taraxacum officinale	12	0.091	-2.398	-0.218
Vinca major	72	0.545	-0.606	-0.331
LID Scenarios				
Achillea millefolium	4	0.021	-3.866	-0.081
Calendula officinalis	8	0.042	-3.173	-0.133
Centaurea cyanus	9	0.047	-3.055	-0.144
Clarkia amoena	3	0.016	-4.154	-0.065
Coreopsis lanceolata	8	0.042	-3.173	-0.133
Coreopsis tintoria	1	0.005	-5.252	-0.027
Cosmos bipinnatus	10	0.052	-2.950	-0.154
Eschscholzia califorica	5	0.026	-3.643	-0.095
Gaillardia pulchella	4	0.021	-3.866	-0.081
Gilia tricolor	1	0.005	-5.252	-0.027
Gypsophilia elegans	9	0.047	-3.055	-0.144
Lupinus perennis	8	0.042	-3.173	-0.133
Ratibida columnaris	9	0.047	-3.055	-0.144
Rudbeckia hirta	10	0.052	-2.950	-0.154
Cheiranthus allioni	10	0.052	-2.950	-0.154
Helianthus annuus	8	0.042	-3.173	-0.133
Echinacea purpurea	6	0.031	-3.461	-0.109
Nemophilia menziesii	7	0.037	-3.306	-0.121
Oenothera lamarckiana	8	0.042	-3.173	-0.133
Papaver rhoeas	8	0.042	-3.173	-0.133
Phacelia tanacetifolia	3	0.016	-4.154	-0.065
Aster novae angliae	8	0.042	-3.173	-0.133
Gaillardia aristata	4	0.021	-3.866	-0.081
Liatris spicata	3	0.016	-4.154	-0.065
Lobularia maritima	0	0.000	0.000	0.000
Monarda fistulosa	6	0.031	-3.461	-0.109
Trifolium incarnatum	4	0.021	-3.866	-0.081

The Shannon-Weiner Index is defined as:

$$H = \sum pi * \ln pi$$

where pi is defined as the proportion of species per area to total species tallied. Additional variables of importance include H_{max} (maximum possible diversity), S, number of species or species richness, and E, species evenness. H_{max} and E are calculated by:

$$H_{max} = \ln S$$

$$E = \frac{H}{H_{max}}$$

Table F-1. Calculated values of Shannon-Weiner Diversity Index.

Base Scenario Existing Biodiversity		LID Scenarios Potential Biodiversity	
Total Samples	132	Total Samples	191
S	5	S	27
H	1.116	H	2.753
H_{max}	1.609	H_{max}	3.296
E	0.693	E	0.835

Appendix E. Rain Garden Runoff Prediction

To determine potential runoff from LID sub-area RG at 610 mm for a 50-yr (180 mm) and 100-yr (201 mm) storm (City of Fayetteville, 2014), Eq. 1 is utilized:

50-yr storm – 180 mm precipitation

$$R = -0.34D + (11.86P - 108)$$
$$= -0.34(610) + (11.86 * 180 - 108)$$
$$= 1{,}819.4\ mm$$

100-yr storm – 201 mm precipitation

$$R = -0.34D + (11.86P - 108)$$
$$= -0.34(610) + (11.86 * 201 - 108)$$
$$= 2{,}068.5\ mm$$

If an engineer or LID professional, instead, was provided target runoff values of less than 1,775 mm for the 50-yr storm and less than 2,025 mm for the 100-yr storm, they would rearrange Eq. 1 and choose the greatest calculated depth to ensure both requirements are met:

50-yr storm – Target Runoff, < 1,775 mm

$$D = \frac{R - (11.86P - 108)}{-0.34}$$
$$= \frac{1{,}775 - (11.86 * 180 - 108)}{-0.34}$$
$$= 741\ mm$$

100-yr storm – Target Runoff, < 2,025 mm

$$D = \frac{R - (11.86P - 108)}{-0.34}$$
$$= \frac{2{,}025 - (11.86 * 201 - 108)}{-0.34}$$
$$= 738\ mm$$

Therefore, to meet both requirements, the rain garden soil depth must be at least 741 mm deep.

Note: these target runoff values were arbitrarily chosen to demonstrate the use of Eq. 1. Additionally, all other rain garden LID sub-area parameters tested in this study must remain unchanged for these equations to remain valid.